

Spontaneous Chirality in Simple Systems

Galen T. Pickett, Mark Gross, and Hiroko Okuyama

Department of Physics and Astronomy, California State University, Long Beach, California 90840
(Received 6 March 2000)

Two simple examples of spontaneous chiral symmetry breaking are presented. The first is close-packed cylindrically confined spheres. As the cylinder diameter is varied, one obtains a variety of chiral phases. The second example involves unconfined dipolar particles with an isotropic attraction, which also exhibits chiral ground states. We speculate that a dilute magnetorheological fluid film, with the addition of smaller particles to provide an attractive entropic interaction, will exhibit a chiral columnar ground state.

PACS numbers: 61.44.-n, 83.80.Gv

The excluded volume interaction is responsible for a remarkable range of collective structures and pattern formation, from solvation shells in simple fluids [1], the crystallization of hard-sphere fluids [2], solvent swelling of polymers [3] and its screening in concentrated solution, and lyotropic liquid crystallinity [4]. These all come about by requiring that no two physical bodies overlap. The excluded volume interaction is thus merely a constraint, which may be supplemented by further constraints, as in films of hard spheres [2,5]. Here we look at structures caused by hard-sphere exclusion and cylindrical confinement on the one hand, and pairwise anisotropic (yet achiral) interactions on the other. In both cases, we find evidence of spontaneous twisting conformations (see Fig. 1), and the spontaneous breaking of *chiral symmetry*. Chirality is all around and even within us. Despite the fact that all atoms and many small molecules are achiral, i.e., there is an improper rotation which maps each to itself, our bodies are filled with chiral organic molecules, and the handedness of each molecule is the same for each and every living creature on Earth. The fact that, e.g., DNA is right-handed is possibly a complicated manifestation of this symmetry breaking [6].

The first model is a hard-sphere fluid at zero temperature, maximally packed into an infinite, hard, and smooth cylinder. Hard spheres ("balls") are packed as densely as possible into the cylinder; effectively they are at infinite pressure. The cylinder axis is along \hat{z} and its diameter is D in units of the ball diameter. The resulting structure has a volume fraction depending only on the degree of confinement, D . For $D = 1$ the balls form a single infinite chain, clearly achiral. For $D \rightarrow \infty$ the balls arrange themselves in one of the two maximum volume-fraction structures, face-centered cubic (fcc) or hexagonal closed-packed (hcp) [2]. (This degeneracy results in neither a pure fcc nor a pure hcp state; next-nearest neighbor interactions can lift this degeneracy and suppress the defects.) These *unconfined* structures are also achiral.

To determine the situation between these two limits, we applied simulated annealing. For fixed D and number of balls N , we determined the smallest length cylinder capable of accommodating all N balls, and thus the maxi-

mal volume-fraction configuration. Increasing N we were able to extrapolate $N, L \rightarrow \infty$ for fixed D . Then D was increased by a small amount and these steps were carried out again. In every case we considered ($1 \leq D \leq 1 + 2/\sqrt{3} \approx 2.155$), the structure was able to be accurately described by identical, staggered, helices of balls in contact with the cylindrical surface. There were relative shifts in azimuthal angle and in z from one helix to another. In

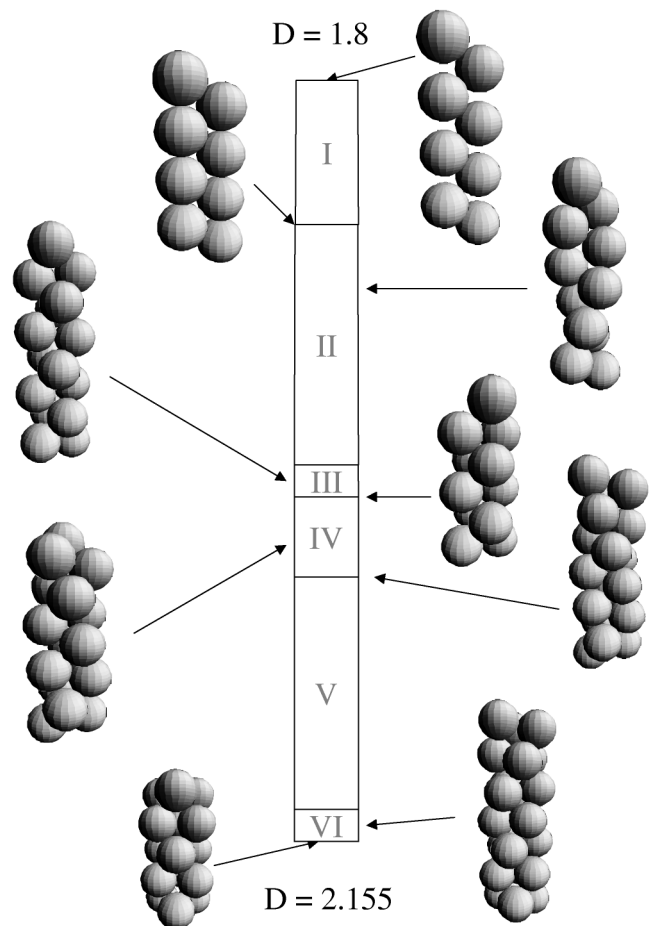


FIG. 1. Close-packed configurations of hard spheres confined inside a cylinder with ratio of diameters given by D . Six phases were found in the range $1 < D \sim 2.155$, five of them chiral.

terms of cylindrical coordinates (ρ_n, z_m, ϕ_n) ,

$$\begin{aligned}\rho_n &= \frac{D-1}{2}, \\ z_n &= na + b, \\ \phi_n &= nc + d,\end{aligned}\quad (1)$$

where n labels balls on the helix, a and c are the same for all balls and for all helices, and b and d vary from one helix to another.

To accelerate convergence in our simulated annealing runs, we allowed the balls to pass through each other with an overlap penalty. As the temperature tended to zero, the penalty suppressed overlap entirely. (This was checked at the end of each run.) The pattern of ball positions was easily identified to be of the form (1), and the parameters were determined from a simple analytic calculation using the linking matrix, i.e., the pattern of interball contacts, determined from the numerical configuration. These values were then checked against the numerical results. As N was increased, the discrepancy between the analytic and numerically obtained parameters decreased, typically to one part in 10^5 away from the ends of the cylinder, where boundary effects were observed. To check that the state of maximum volume fraction had indeed been reached, we repeated the simulations many times with no states of higher volume fraction appearing. An additional experimental but qualitative check involved placing small uniform balls in a cylinder and shaking the cylinder until order appeared.

Figure 1 shows these closed-packed structures in the range $1.8 \leq D \leq 1 + 2/\sqrt{3}$. There were six distinct phases found; between each some derivative of the volume fraction with respect to D is discontinuous. The achiral phase from $1 \leq D \leq 1 + \sqrt{3}/2 \approx 1.866$ (I) consists of a zigzag planar arrangement of balls which can also be described as a single helix such that the change of azimuthal angle from one ball to the next is equal to π . This phase is, of course, achiral. At $D = 1 + \sqrt{3}/2$ the gaps between the next-nearest neighbor balls vanish. To maintain maximum volume fraction with $D \gtrsim 1 + \sqrt{3}/2$, the third ball falls off to the left or to the right with respect to the first, determining the chirality. Although the chiral phase from $1 + \sqrt{3}/2 < D < 1 + 4\sqrt{3}/7 \approx 1.99$ (II) appears to consist of two helices winding around each other, it can be described algebraically as a single helix. This is no longer the case for $1 + 4\sqrt{3}/7 < D < 2$ (III), which consists of two staggered helices. $D = 2$ is an isolated case consisting of achiral "doublets." The phases $2 < D < 1 + 3\sqrt{3}/5 \approx 2.04$ (IV) and $1 + 3\sqrt{3}/5 < D \leq 2.14$ (V) are also described algebraically by two staggered, identical helices but are distinguished by the "linking pattern," i.e., the pattern of contact neighbors of each ball. The state from $2.14 \leq D < 1 + 2/\sqrt{3} \approx 2.155$ (VI) is described algebraically by three staggered, identical helices. Finally, at $D = 1 + 2/\sqrt{3} \approx 2.155$ there is an isolated achiral "triplet" state. We did not proceed beyond $D \approx 2.155$.

Each of the chiral configurations shown in Fig. 1 is one of a pair of structures with opposite handedness. Each handedness appears roughly half the time in our simulations, and both have the same volume fraction. This is the nature of the spontaneous symmetry breaking of chiral symmetry, demonstrated here in the *incompressible limit* of the hard-core, cylindrically confined solid.

Figure 2 shows the volume fraction as a function of D over approximately the same range as Fig. 1. At any D , it is *impossible* to fill the cylinder more densely with spheres. Any increase in the internal sphere density violates *some* hard-core constraint in the system. Four of the five structural transitions are clearly evident as cusps; the one at $D = 1 + 4\sqrt{3}/7 \approx 1.99$ is not as obvious. For reference, the volume fraction of fcc and hcp phases is approximately 0.74.

Figure 3 presents a chiral order parameter, $\xi(D)$ that is a cousin of one derived by Harris, Kamien, and Lubensky [7]. Defining $\rho_{lm} = \sum_i Y_{lm}(\theta_i, \phi_i)$ [as in their Eq. (9) but without the factors of $|r_i|$], where i labels the balls and the Y_{lm} are spherical harmonics, we let $\Psi_{l_1 l_2 L} \equiv \sum_{mn} C(l_1 l_2 L; mn) \rho_{l_1, m} \rho_{l_2, n} \rho_{L, m+n}^*$, with the $C(l_1 l_2 L; mn)$ appropriate Clebsch-Gordan coefficients (see [7]). Specifically, we define $\xi \equiv \sqrt{|\Psi_{234}^2| + |\Psi_{346}^2| + |\Psi_{456}^2|}$. This choice is certainly not unique, but does have the property that $\xi > 0$ implies that the structure is chiral, and the size of ξ measures the *amount* of chirality. Figure 3 shows that the only achiral states in the range studied are the achiral doublet and achiral triplet states at $D = 2$ and $D = 1 + 2/\sqrt{3}$, respectively. The discontinuity in ξ at $D \approx 2.14$ accompanies a discontinuous change in structure.

There might be physical applications of the structures discovered here. For example, typical nanotubes have inner diameters of 3–6 nm, and methods for filling them with various molecules and even small crystals have been available for some time [8]. By packing a nanotube with weakly interacting molecules or a mesoscopic tubule with weakly interacting colloids, chiral structures including

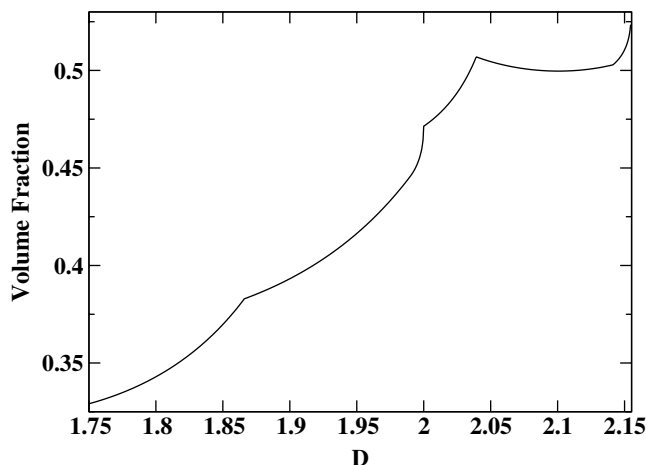


FIG. 2. Volume fraction as a function of D .

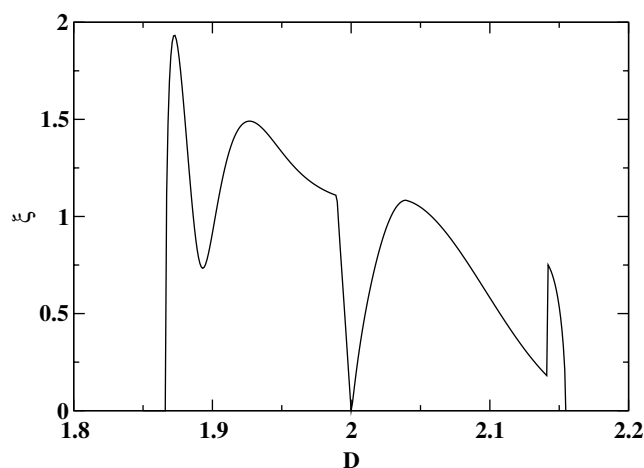


FIG. 3. Chiral order parameter as a function of D . Here we plot the chiral order parameter, ξ , defined in the text, vs the degree of confinement, D , for cylindrically confined hard spheres. In all cases, ξ was calculated for 15 consecutive spheres in the analytically determined close-packed structure. The structures are achiral ($\xi = 0$) only for $D \leq 1 + \sqrt{3}/2$, for $D = 2$, and for $D = 1 + 2/\sqrt{3}$.

chiral filters might be constructed with precisely designed properties. Such chiral filters could be of use in the physical separation of enantiomers, and facilitate the inorganic synthesis of bioactive compounds [9].

It turns out that packing models similar to the one discussed above are found in the literature of phyllotaxis, the study of helical patterns in sunflowers, pineapples, pine cones, etc. [10]. In Ref. [10], however, it was *assumed* that the closest packing state could be described mathematically by a single helix, which is not generally the case. Also, when D becomes large enough so that not every sphere in the close-packed configuration is in contact with the cylinder surface, all contact with the cylinder phyllotaxis models is lost. We have not carried out simulations to such large D , however.

The other model we consider in this paper consists of hard-sphere particles with embedded dipole moments all held parallel to the z axis, and short-ranged attractive interactions,

$$U = U_{\text{hard sphere}} + U_{\text{dipole}} + U_{\text{attr}}. \quad (2)$$

An approximate example of such a system consists of magnetorheological (MR) particles with additional short-ranged, attractive interactions generated by the addition of smaller particles [11]. In the absence of boundaries, setting $U_{\text{attr}} = 0$ in (2) for less than 30 particles gives a ground state consisting of all the available particles forming a single straight chain along the z axis. $U_{\text{attr}} \neq 0$ tends to break the chain and cause columns to form. Through numerical simulations we have found that a certain range of choices for U_{attr} results in ground states which consist of helices of particles similar to those in Fig. 1. The particles thus arrange themselves to have more neighbors, lowering the energy of the system.

We have tried a variety of models for the short-ranged interaction, but present only one class here. For simplicity we work in units for which the ball diameter and the dipole moment of the particles are set equal to 1. As a function of the distance between two balls, r , let the pairwise attractive potential be

$$U_{\text{attr}}(r) = \begin{cases} -\epsilon \frac{R-r}{R-1}, & 1 \leq r \leq R \\ 0, & \text{otherwise} \end{cases}, \quad (3)$$

with $\epsilon \geq 0$ and $R \geq 1$ controlling the strength and range of the interaction. Here $U_{\text{dipole}} = \frac{r^2 - 3z^2}{r^{5/2}}$ if the particles are separated by z in the dipole direction. The model has no chiral interactions and no boundary conditions. The simulations described here were carried out with 15 balls. Using this small number made it feasible to find the exact ground state for many different choices of ϵ and R by simulated annealing, despite the presence of an extremely rough energy landscape.

Let us first examine the limiting cases. For $\epsilon \rightarrow 0$ the attractive interaction is turned off, and the ground state is a single achiral chain, independent of R . For $\epsilon \rightarrow \infty$ the dipolar interaction is turned off and an achiral cluster is obtained, for all R . For $R \rightarrow \infty$ the attractive interaction is a constant for nonoverlapping particles, independent of ϵ , and we are back to the single achiral chain. Thus any chiral phase must occur between these extremes.

Figure 4 shows the approximate phase diagram for 15 balls, exhibiting a region of chiral ground states. Most of these states consist of three chains winding around each other, with the number of balls in each chain and the detailed structure varying with the parameters ϵ and R . Thus, we suggest that if one adds excess surfactant (or other small particles) to a dilute MR fluid film [11], a chiral columnar phase may appear within a range of

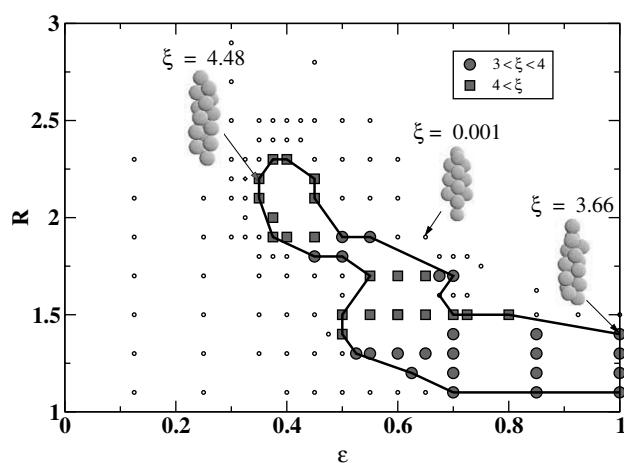


FIG. 4. Range of potentials of the form (2) and (3), in which spontaneous chiral symmetry breaking occurs. Three sample sphere configurations are indicated (two chiral, one achiral). The bold line contains all the chiral states, and is merely meant to guide the eye. The tiny open circles indicate achiral states as determined by simulation. The size of the chiral order parameter is roughly indicated.

parameters. Our purpose in specifying films, rather than unconfined droplets, is simply to keep the columnar clusters finite. It is interesting to note that some chiral MR columns have been observed in simulations and experiments [12,13], but there is no evidence that these were metastable [12]. It is therefore probable that the ground state of an MR fluid film is chiral only in the presence of an additional attractive interaction.

One might criticize the relevance of our two models to chiral symmetry breaking, as follows. The first model is one dimensional, and therefore exhibits a symmetry-breaking phase transition only in the unphysical limit of infinite pressure or zero temperature. The second model, with a single cluster, involves only a finite number of particles, and hence no true phase transition is possible. While these statements are certainly true, one can easily define a chiral correlation length in terms of a local version of the order parameter ξ (above). Real systems are, in fact, finite, and if the chiral correlation length exceeds the size of the system, spontaneous chirality will occur, at whatever temperature. This is presumably how chiral molecules such as amino and nucleic acids form naturally from essentially achiral atoms. Furthermore once chiral clusters are formed, intercluster interactions will in general depend on whether the clusters have the same or different chirality. Thus, if these chiral building blocks are tightly bound, one can get extended chiral phases in two and three dimensions, for example, in chiral nematic and cholesteric liquid crystals, and perhaps in the modified MR fluid film described above.

We speculate that many examples of spontaneous chiral symmetry breaking in physical systems at the molecular and the mesoscopic scale are a result of competing interactions or boundary effects, similar to those associated with the models discussed here. One possible example involves the synthesis of polyisocyanates. These helical homopolymers can be synthesized with no intrinsic (chemical) chirality, yet nevertheless spontaneously form left- and right-handed helices [14]. Another possible example involves chiral tubule phospholipids which in their initial stages form ribbonlike structures in a manner compatible with chiral symmetry breaking [15]. Although the large molecular building blocks in this example have a small chiral component, roughly equal numbers of left- and right-handed inner tubule layers form. It is therefore likely that the chirality of the building blocks play little role in this initial and rapid stage of tubule formation, and the origin of the chirality is spontaneous symmetry breaking due to packing and/or interactions.

The authors thank Randall Kamien, Jing Liu, James E. Martin, Britt Thomas, and Thomas Witten for helpful discussions. This work was supported in part by National Science Foundation Grant No. DMR-9803618 and the California State University.

Note added.—While making final revisions, three relevant papers have come to our attention, two of them

published very recently. In Ref. [16], simulations are presented that suggest that extremely thin aluminum and lead wires could be chiral, and in Ref. [17], chiral gold wires are experimentally realized. In Ref. [18], evidence of intense optical activity in small gold clusters is presented. We feel that our work provides additional evidence of the ubiquitous nature of such chiral states due to packing and/or a variety of achiral interactions.

-
- [1] J. P. Hansen and I. R. McDonald, *Theory of Simple Liquids* (Academic, London, 1986).
 - [2] M. Schmidt and H. Lowen, *Phys. Rev. E* **55**, 7228 (1997).
 - [3] P.-G. de Gennes, *Scaling Concepts in Polymer Physics* (Cornell University Press, Ithaca, 1979).
 - [4] D. Frenkel, in *Liquids, Freezing, and Glass Transition*, Proceedings of the Les Houches Summer School, Session L1, edited by J. P. Hansen, D. Levesque, and J. Zinn-Justin (Elsevier B.V., Amsterdam, 1991); G. J. Vroege and H. N. W. Lekkerkerker, *Rep. Prog. Phys.* **55**, 1241 (1992).
 - [5] S. Granick, *Phys. Today* **52**, No. 7, 26 (1999).
 - [6] The intrinsically chiral parity-violating weak interactions have been suggested as an alternative explanation for the existence of chirality in the macroscopic world. It should be kept in mind, however, that this extremely feeble nuclear effect is very weakly coupled to chemistry. To the best of our knowledge there has not yet been any measurements of chemical properties of atoms or molecules, for example, energy levels, reaction rates, etc., where electroweak parity violation plays any discernible role. This weak effect could, of course, bias a *spontaneous breaking* of chiral symmetry and thus assist in the global prebiotic stereoselection of right-handed nucleic acids and left-handed amino acids during biogenesis. See D. C. Walker, *Orig. Life* **7**, 383 (1976); L. Keszthelyi, *Nature (London)* **219**, 197 (1976).
 - [7] A. B. Harris, R. D. Kamien, and T. C. Lubensky, *Rev. Mod. Phys.* **71**, 1745 (1999).
 - [8] S. C. Tang, Y. K. Chen, P. J. F. Harris, and M. L. H. Green, *Nature (London)* **372**, 159 (1994).
 - [9] T. E. Grier, X. Bu, P. Feng, and G. D. Stucky, *Nature (London)* **395**, 154 (1998).
 - [10] L. S. Levitov, *JETP Lett.* **54**, 546 (1991); *Europhys. Lett.* **14**, 533 (1991).
 - [11] A. D. Dinsmore, A. G. Yodh, and D. J. Pine, *Nature (London)* **383**, 239 (1996).
 - [12] J. E. Martin, R. A. Anderson, and C. P. Tigges, *J. Chem. Phys.* **108**, 3765 (1998).
 - [13] J. Liu (private communication).
 - [14] M. M. Green, N. C. Peterson, T. Sato, A. Teramoto, R. Cook, and S. Lifson, *Science* **268**, 1860 (1995).
 - [15] B. Thomas, C. M. Lindemann, and N. A. Clark, *Phys. Rev. E* **59**, 3040 (1999).
 - [16] O. Gulseren, F. Ercolelli, and E. Tosatti, *Phys. Rev. Lett.* **80**, 3775 (1998).
 - [17] Y. Kondo and K. Takayanagi, *Science* **289**, 606 (2000).
 - [18] T. G. Schaaff and R. L. Whetten, *J. Phys. Chem. B* **104**, 2630 (2000).